PHYSICAL REVIEW B VOLUME 57, NUMBER 14 1 APRIL 1998-II

Electric-field-gradient analysis of high-T_c superconductors

Ivan Kupčić and Slaven Barišić
Department of Physics, POB 162, Faculty of Sciences, University of Zagreb, Zagreb, Croatia

Eduard Tutiš
Institute of Physics of the University, POB 304, Zagreb, Croatia

(Received 26 June 1997; revised manuscript received 7 October 1997)

The qualitative and quantitative features of the electronic charge distribution in cuprate superconductors are reexamined on the basis of a comprehensive set of nuclear quadrupole resonance and NMR measurements. A systematic analysis of measured electric-field gradients is performed within the tight-binding approach, commonly used for electronic models in cuprates. Both in-plane and out-of-plane sites and orbitals are considered. Special attention is given to the generic pd model involving only the σ orbitals in the CuO_2 planes. This model is checked against the experimental data. The physical origin of several material-dependent features is clarified. It is shown that in $La_{2-x}Sr_xCuO_4$ the $3d_{3z^2-r^2}$ orbital of the in-plane copper and the $2p_z$ apex oxygen orbital are occupied by a substantially smaller fraction of holes than the in-plane σ orbitals, at variance with proposals lending importance to copper-apex oxygen hybridization. At the in-plane oxygen site a sizable $2p_z$ admixture is found at the Fermi level of $YBa_2Cu_3O_7$. The in-plane charge distribution of $Tl_2Ba_2CuO_4$ is found to be qualitatively similar to that of the high-temperature tetragonal phase of $La_{2-x}Sr_xCuO_4$. It appears that the additional holes are shared among copper and oxygen sites in similar proportions. This is shown to be compatible with the large U_d Emery model provided that the difference between the p and d atomic energies is comparable to the first neighbor overlap energy. [S0163-1829(98)03914-9]

I. INTRODUCTION

The charge and spin distributions in layered cuprates, as well as the relations between these two distributions, have been intensively studied by various experimental methods, for a wide range of dopings.[1–10] The NMR and nuclear quadrupole resonance (NQR) studies of both antiferromagnetic and metallic compounds contributed significantly to the understanding of this matter, measuring the electric-field gradients (EFG's) at nuclear positions, and being very sensitive to the formation of the local spins.

There are several materials for which EFG's are rather completely investigated. More precisely, in these materials the components of the traceless EFG tensor are well known for all ions with a partially occupied outer shell.[1–4,11,12] In some cases, even the dependence of EFG's on doping is established.[4,8,13]

The theoretical analysis of the EFG data followed several routes. For example, Schwarz *et al.*[14] calculated the electric-field gradients of the $YBa_2Cu_3O_{7-x}$ family in a first-principles approach, using the local-density approximation. Good agreement with experimental EFG's is found. However, the basis of three or more valence subshells per crystal site (e.g., $3d$, $4s$, and $4p$ orbitals at the copper site) is too wide, and the local-density approximation is too crude to give results which can be simply related to those commonly obtained in electronic many-body models. On the other hand, Shimizu[15] has studied the EFG at copper sites in various high-T_c cuprates including from the outset only the $3d_{x^2-y^2}$ valence orbital on the copper ion. The effects of quadrupolar polarizability on the charge distribution were described through the Sternheimer antishielding factor γ, as usual. However, Shimizu did not take into account the intersite hybridization between the valence orbitals. This was further considered by Hanzawa *et al.*[16] However, being interested only in the EFG at the in-plane ions, Hanzawa *et al.* simplified the model by omitting the contribution of the quadrupolar polarizability to the EFG. In this paper, we present a complete quantitative analysis of the electric-field gradients based on the tight-binding picture. Such an approach provides a link between the EFG measurements and the many-body models based on the tight-binding approximation, usually used for most theoretical considerations of high-T_c cuprates. A reasonable balance between the accuracy on the single particle level and the accuracy in the treatment of the strong electronic correlations is achieved in this way. We estimate that our calculations are performed with one in ten accuracy. The relevance of various valence orbitals as well as the effects of the quadrupolar charge polarizability on EFG's for several representative members of the high-T_c superconductors (HTSC's) is considered in this spirit.

The complete information on EFG's proves very useful when resolving the question of the charge distribution among various ions and their orbitals. The main advantage of this analysis comes from the possibility to distinguish among local and lattice contributions to EFG's. The local charge distribution is related to partially filled orbitals at the ion considered, while the lattice charge distribution relates to other neighboring sites (ions). Furthermore, the local part is usually extremely sensitive to how charge is shared among local orbitals. Therefore, the investigation of the EFG at various nuclei in the layered cuprates may give rather precise information on the symmetry of the atomic orbitals which build up the valence bands (see Sec. III).[17] The important questions that may be answered in this way, out of several others to be discussed, are as follows.

(i) The relative importance of $3d_{x^2-y^2}$ and $3d_{3z^2-r^2}$ copper orbitals in hosting the extra charge introduced by doping. This can be inferred from the existing EFG data and the fact that local contributions of $3d_{x^2-y^2}$ and $3d_{3z^2-r^2}$ orbitals are opposite in sign.

(ii) The amount in which the $2p_z(\pi)$ orbital is admixed to the $2p_\sigma$ orbital of the in-plane oxygen ion. The admixture, breaking the uniaxial symmetry of EFG, becomes the subject of easy observation.

(iii) The effect of doping on the apex oxygen. Some theories attribute an important role to the hybridization between copper $3d_{x^2-y^2}$ and apex-oxygen $2p_z$ orbitals. This question can be readily addressed by studying the symmetry of EFG at the apex oxygen site.

The EFG data obtained in the $La_{2-x}Sr_xCuO_4$ family will be our major interest. The reason for that lies in the relative simplicity of this compound, as well as in the fact that the doping dependencies of NMR and NQR spectra in $La_{2-x}Sr_xCuO_4$ are well established. In addition, we will discuss the results available for $YBa_2Cu_3O_7$ and $Tl_2Ba_2CuO_6$.

Finally, in Sec. IV the in-plane charge distribution is analyzed within the framework of the Emery pd model. We show that the model with strong Coulomb repulsion U_d on the in-plane copper site accounts well for the doping dependence and the size of the observed EFG's, provided the dimensionless parameter t_{pd}/Δ_{pd} is chosen to be of the order of unity.

II. THEORETICAL ANALYSIS OF EFG'S

In materials where the spherical symmetry of the on-site charge distributions is broken (HTSC materials being an example), the nuclear resonant frequencies of the nuclei with spin $I>1/2$ are strongly affected by the nuclear quadrupole interaction between the nuclear quadrupole moments Q and electric field gradients $V_{\alpha\alpha}$. By measuring the resonant frequencies it is possible to find the values of these gradients. Indeed, strong electric field gradients were measured at almost all crystal positions in the materials under consideration.[1–4,11,12] It has been shown previously that in some cases the EFG is dominanted by the contribution of the on-site charges,[16] reflecting the effects of the intra-atomic and interatomic hybridization among the outermost orbitals, while in some other cases the contributions of the surrounding ions dominate.[15] To take both of these possibilities into account, we start our EFG analysis with the expression

$$V_{\alpha\alpha}=V_{\alpha\alpha}^{\text{local}}-\sum_{\beta} R_{\alpha\beta}V_{\beta\beta}^{\text{local}}+V_{\alpha\alpha}^{\text{lattice}}-\sum_{\beta} \gamma_{\alpha\beta}V_{\beta\beta}^{\text{lattice}}. \quad (1)$$

An expression similar to Eq. (1) was originally derived for ionic insulators where R and γ reduce to scalars.[18] Various simplifications of this, already simplified, equation have been used previously for the explanation of the EFG's in the HTSC materials.[15,16] However, our purpose, to analyze carefully most of the available experimental results, compels us to use it in its general form, including explicitly the effect of hybridization among the outermost orbitals on $V_{\alpha\alpha}$.

The structure of Eq. (1) can be easily understood from the following tight-binding reasoning. As usual for HTSC materials, we choose the hole picture to describe the electronic degrees of freedom. The corresponding *vacuum* state comprises the ions with closed outermost subshells Cu^{1+}, O^{2-}, La^{3+}, Ba^{2+}, Y^{3+}, and Tl^{1+}. The crystal field V^{lattice} acts on the on-site charge distribution in different ways. The intra-atomic hybridizations arise from multipole terms of the crystal field whereas different interatomic hybridizations and electron-electron interactions modify the on-site charge distribution, resulting finally in the expression for the total electronic charge on a site

$$-2e\sum_{nl\kappa}(1-n_{nl\kappa})|\Psi_{nl\kappa}|^2. \quad (2)$$

Here $n_{nl\kappa}$ is the number of holes per spin in the orbital characterized by quantum numbers n, l, and κ. $\Psi_{nl\kappa}$ is the corresponding wave function. V^{lattice} affects both $\Psi_{nl\kappa}$ and $n_{nl\kappa}$ (by shifting and splitting the related orbital energy levels). Note that even small energy splittings, associated with symmetry breaking induced by the crystal field, result in large charge redistributions among the orbitals at the considered site. Similar redistributions among sites are associated with the intersite hybridization. However, once the symmetry of the energy splitting is established, the value of V^{lattice} influences primarily $\Psi_{nl\kappa}$ while the effect on $n_{nl\kappa}$ is relatively small.

In order to factorize Eq. (2) in a way useful to the EFG analysis we write the quadrupolar corrections in $\Psi_{nl\kappa}$ explicitly

$$-2e\sum_{nl\kappa}(1-n_{nl\kappa})[(\Psi_{nl\kappa}^0)^2+2\Psi_{nl\kappa}^0\delta\Psi_{nl\kappa}^{\text{lattice}} +2\Psi_{nl\kappa}^0\delta\Psi_{nl\kappa}^{\text{local}}]. \quad (3)$$

$\delta\Psi_{nl\kappa}^{\text{lattice}}$ and $\delta\Psi_{nl\kappa}^{\text{local}}$ represent, respectively, the polarizations of the orbital $\Psi_{nl\kappa}^0$ by the quadrupolar part of the crystal potential of the surrounding ions, and by the quadrupolar part of the local electron-electron interactions due to redistribution of the local charge. As can be easily seen, the corresponding effect of the dipolar term on EFG can be absorbed in the variation of $n_{nl\kappa}$. $\Psi_{nl\kappa}^0$ may be factorized in the usual way using the normalized radial and angular part of the wave function $\Psi_{nl\kappa}^0=R_{nl}(r)f_{l\kappa}(\Omega)$. The function $f_{l\kappa}(\Omega)$ is the real combination of the spherical harmonics $Y_{lm}(\Omega)$ with the same l (with average components of the orbital angular momentum equal to zero). It is an appropriate starting point for the tight-binding description of the charge carriers in a crystal. Thus, after putting the whole charge acting on a given nucleus into the expression for EFG, one obtains

$$V_{\alpha\alpha}=\int d^3r\frac{3r_\alpha^2-r^2}{r^5}\Bigg\{2e\sum_{nl\kappa} n_{nl\kappa}(\Psi_{nl\kappa}^0)^2 -2e\sum_{nl\kappa}(1-n_{nl\kappa})2\Psi_{nl\kappa}^0\delta\Psi_{nl\kappa}^{\text{local}}+\rho^{\text{lattice}} -2e\sum_{nl\kappa}(1-n_{nl\kappa})2\Psi_{nl\kappa}^0\delta\Psi_{nl\kappa}^{\text{lattice}}\Bigg\}. \quad (4)$$

Here ρ^{lattice} is the charge distribution from the surrounding ions. Since any distribution $n_{nl\kappa}$ of holes over orbitals which

results in a spherical on-site charge distribution (in particular the filled subshells) does not contribute to the EFG, the contribution of $-2e\Sigma_{nl\kappa}(\Psi^0_{nl\kappa})^2$ is absent in Eq. (4).

The four parts of Eq. (4) correspond to the four contributions already separated in Eq. (1). Two of these are direct ones,

$$V^{\rm local}_{\alpha\alpha}=\int d^3r\frac{3r_\alpha^2-r^2}{r^5}2e\sum_{nl\kappa}\ n_{nl\kappa}(\Psi^0_{nl\kappa})^2, \tag{5}$$

$$V^{\rm lattice}_{\alpha\alpha}=\int d^3r\frac{3r_\alpha^2-r^2}{r^5}\rho^{\rm lattice}, \tag{6}$$

and two are indirect,

$$\sum_\beta\ R_{\alpha\beta}V^{\rm local}_{\beta\beta}=\int d^3r\frac{3r_\alpha^2-r^2}{r^5}2e\sum_{nl\kappa}\ (1-n_{nl\kappa})\times 2\Psi^0_{nl\kappa}\delta\Psi^{\rm local}_{nl\kappa}, \tag{7}$$

$$\sum_\beta\ \gamma_{\alpha\beta}V^{\rm lattice}_{\beta\beta}=\int d^3r\frac{3r_\alpha^2-r^2}{r^5}2e\sum_{nl\kappa}\ (1-n_{nl\kappa})\times 2\Psi^0_{nl\kappa}\delta\Psi^{\rm lattice}_{nl\kappa}, \tag{8}$$

with corresponding shielding tensors R and γ. Equations (7) and (8) describe in particular the case considered here, when the crystal field splittings and/or the hybridization effects between outer orbitals result in only one of orbitals at given site, the σ one, to be occupied by holes. Then R is a scalar, while γ remains a tensor. Note that large values of γ can correspond to small ionic polarizabilities $\delta\Psi^{\rm lattice}_{nl\kappa}$ because at short distances the effect of $\delta\Psi^{\rm lattice}_{nl\kappa}$ on γ is enhanced by the singularity in the nuclear quadrupole interaction.[19]

In following subsections we outline the procedure to be used in the analysis of all four contributions to EFG. The part of the analysis related to particular sites in HTSC compounds and particular sets of data will be carried out in Sec. III. For this sake we introduce here a few customary notions and abbreviations.

In order to introduce the frequency scale associated with EFG's, one defines auxiliary frequencies

$$\nu_{aa}=\frac{3}{2I(2I-1)h}eQV_{aa}, \tag{9}$$

where I is the nuclear spin.

For nuclei with spin $I=3/2$ in the nuclear quadrupole resonance experiments the nuclear resonant frequency is usually labeled by ν_Q and is equal to

$$\nu_Q=|\nu_{\gamma\gamma}|\sqrt{1+\eta^2/3}. \tag{10}$$

The asymmetry parameter η in Eq. (10) is conventionally defined as

$$\eta=\frac{V_{\alpha\alpha}-V_{\beta\beta}}{V_{\gamma\gamma}}, \tag{11}$$

where the local axes α, β, and γ are chosen so that $0\leqslant\eta\leqslant 1$.

A. Direct lattice contribution

The contribution of Eq. (6) is first calculated in the point charge approximation

$$V^{\rm lattice}_{\alpha\alpha}=\sum_i\ q_i\frac{3R^2_{\alpha i}-R_i^2}{R_i^5}. \tag{12}$$

Here q_i is the effective charge of the ith ion, and $\mathbf{R}_i$ is its position. The sum goes over all crystal sites except for the one considered. Various departures of real lattices from the idealized planar ones are taken into account by using the crystallographic data from Refs. 20–22. For example, the buckling of CuO_2 planes in $YBa_2Cu_3O_7$ and the displacement of ions in TlO planes from their ideal positions in $Tl_2Ba_2CuO_6$ are included.

Although the point charge approximation in the calculation of $V^{\rm lattice}_{\alpha\alpha}$ is a reasonable one, the leading corrections to the values obtained by Eq. (12) are also estimated. The latter originate from a more realistic description of the distribution of holes over σ orbitals in the close neighborhood of the considered site. Using Slater-type wave functions, we find that $V^{\rm lattice}_{\alpha\alpha}$ and the asymmetry parameter η remain unchanged by such corrections with an accuracy of 1 part in 10. This question is taken up again in Sec. III B.

B. Direct local contribution

When only the σ orbital is occupied by hole at the site considered, the direct local contribution $V^{\rm local}_{\alpha\alpha}$ is

$$V^{\rm local}_{\alpha\alpha}=2n_{nl\kappa}eC^{l\kappa}_{\alpha\alpha}\langle 1/r^3\rangle_{nl}, \tag{13}$$

according to Eq. (5). Here $2n_{nl\kappa}$ is the average number of holes in the orbital and

$$\langle 1/r^3\rangle_{nl}=\int r^2drR^2_{nl}\frac{1}{r^3},$$

$$C^{l\kappa}_{\alpha\alpha}=4\pi\int d\Omega f^2_{l\kappa}(\Omega)f^2_{p\alpha}(\Omega)-1. \tag{14}$$

In the factorization of expression (13) the relation $r_\alpha=\sqrt{4\pi/3}f_{p\alpha}r$ is used. Unlike some earlier approaches to the HTSC materials, when $\langle 1/r^3\rangle_{3d}$ for Cu ions and $\langle 1/r^3\rangle_{2p}$ for O ions were treated as free parameters, to be estimated from the experimental EFG's for each material separately,[16] we assume that these parameters have the same values for all materials considered, which in addition can be significantly different from their values for free ions/atoms. Actually, we take over the estimates of $\langle 1/r^3\rangle_{nl}$ from previous Knight shift analysis in $YBa_2Cu_3O_7$,[2,3] $\langle 1/r^3\rangle_{2p}=3.75$ a.u., and $\langle 1/r^3\rangle_{3d}=6$ a.u. Note that these values can be expressed in terms of the Slater-type wave functions[23] for the electrons in the $2p$ oxygen and $3d$ copper orbitals

$$\langle 1/r^3\rangle_{2p}=\frac{1}{24}\left(\frac{\zeta_{2p}}{a_0}\right)^3,$$

$$\langle 1/r^3\rangle_{3d}=\frac{1}{405}\left(\frac{\zeta_{3d}}{a_0}\right)^3, \tag{15}$$

TABLE I. The factors $C_{\alpha\alpha}^{l\kappa}$ for the orbitals with p and d symmetry.

orbital	$C_{\alpha\alpha}^{l\kappa}$	$C_{\beta\beta}^{l\kappa}$	$C_{\gamma\gamma}^{l\kappa}$
$d_{\alpha^2-\beta^2}$	2/7	2/7	−4/7
$d_{\alpha\beta}$	2/7	2/7	−4/7
$d_{\alpha\gamma}$	2/7	−4/7	2/7
$d_{\beta\gamma}$	−4/7	2/7	2/7
$d_{3\gamma^2-r^2}$	−2/7	−2/7	4/7
p_α	4/5	−2/5	−2/5
p_β	−2/5	4/5	−2/5
p_γ	−2/5	−2/5	4/5

where $\zeta_{2p}=4.48$ and $\zeta_{3d}=13.44$ are the corresponding effective charges of the nuclei for these two orbitals (not simply related to q_i), and a_0 is the Bohr radius.

One of the most interesting questions concerning the charge distribution in the HTSC materials is the rate of admixing the π orbitals to the σ ones at oxygen and copper in-plane ions. This can be answered using the values of the factors $C_{\alpha\alpha}^{l\kappa}$ for p and d orbitals given in Table I. Note in this respect that the contributions of the outer orbitals at the same ion are distinguished by symmetry, except for the case of $d_{\alpha^2-\beta^2}$ and $d_{\alpha\beta}$ orbitals, since the latter have the same axial symmetry, and the factors $C_{\alpha\alpha}^{l\kappa}$ have the same sign. Two issues can therefore be meaningfully addressed here: (i) the admixture of the $2p_z$ orbital to the corresponding σ orbital at the oxygen positions, and (ii) the admixture of the $3d_{3z^2-r^2}$ to the $3d_{x^2-y^2}$ orbital at the copper positions. Leaving the details of the analysis for Sec. III, it may be mentioned here that in the case (i) the occupation of the $2p_z$ oxygen orbital can be directly estimated from the symmetry of the local contribution to EFG, provided that the local contribution is suitably extracted from the experimental data. On the other hand, for the $3d_{3z^2-r^2}$ and $3d_{x^2-y^2}$ orbitals the factors $C_{\alpha\alpha}^{l\kappa}$ are opposite in sign, and it is possible to distinguish the respective contributions of those orbitals by changing the total charge on the copper ions.

C. Indirect contributions

The expressions for the indirect contributions to EFG are given by Eqs. (7) and (8). It is important to remember that for ionic insulators, i.e., when holes are absent, γ itself reduces to a scalar. This is relevant here for the cases when the ionic configuration in the crystal results from polarizing the closed shells of an ion. For example, this occurs on the in-plane O sites in La_2CuO_4 and $YBa_2Cu_3O_6$ when the Cu-O hybridization is negligible. In addition, γ is a scalar when there is a fourfold symmetry axis at the site considered. This is easily understood on noting that both $V_{\alpha\alpha}$ and $V_{\alpha\alpha}^{\rm lattice}$ have to satisfy the Laplace equation. Such is the case at the Cu site in HTT phase of $La_{2-x}Sr_xCuO_4$.

Let us first mention the earlier relevant results. The indirect contributions to EFG in the closed-shell-ion cases have been intensively studied by Sternheimer. He obtained $\gamma(\mathrm{O})=-4.1$, $R(\mathrm{O})=0.078$ and $\gamma(\mathrm{Cu}^{1+})=-15.46$, $R(\mathrm{Cu}^{1+})=0.179$.[19]

Since factors R enter in Eq. (1), or below in Eq. (17), only through the product $(1-R)\langle 1/r^3\rangle$, the values of these two factors cannot be discussed separately, so that for $R(\mathrm{O})$ and $R(\mathrm{Cu})$ we use the approximate theoretical values 0.1 and 0.2, respectively.

In this subsection we consider the effect of interatomic hybridization on γ. First we recall Sternheimer's general result that in the closed-shell-ion case the dominant contribution to γ arises from the *radial* polarization of the outermost p orbitals.[19] This term is usually labeled by $\gamma(np\rightarrow p)$. It is thus expected that the largest tensorial corrections to γ in the HTSC materials will appear at the oxygen in-plane ions as a result of the interatomic hybridization. In order to estimate these tensorial corrections, we generalize Sternheimer's calculation for radial quadrupolar polarizability of p orbitals to situations with fractional occupation numbers $n_{nl\kappa}$. This is done in the Appendix.

Note that the definition of γ by Eq. (8) is not unique because $V_{\alpha\alpha}^{\rm lattice}$ satisfies the Laplace equation. Therefore, any term proportional to $\Sigma_\alpha V_{\alpha\alpha}^{\rm lattice}$ can be added to the left-hand side of Eq. (8). We use this freedom to minimize the off-diagonal components of γ.

Unlike the case of closed shells, for fractional occupation numbers the off-diagonal components of $\gamma(np\rightarrow p)$ cannot be simultaneously taken to zero by using the Laplace equation. As shown in the Appendix the overall $\gamma(np\rightarrow p)$ can be then expressed as

$$\gamma(np\rightarrow p)=\gamma^0(np\rightarrow p)+\delta\gamma(np\rightarrow p), \tag{16}$$

where $\gamma_0(np\rightarrow p)=48/25I_{np}$, in accordance with the Sternheimer's result and the tensorial content of $\gamma(np\rightarrow p)$ comes through $\delta\gamma(np\rightarrow p)$:

$$\delta\gamma_{zz}(np\rightarrow p)=-\frac{8}{25}(4n_{npz}+n_{npx}+n_{npy})I_{np},$$

$$\delta\gamma_{zx}(np\rightarrow p)=\frac{8}{25}(n_{npx}-n_{npy})I_{np},$$

$$\delta\gamma_{zy}(np\rightarrow p)=\frac{8}{25}(n_{npy}-n_{npx})I_{np}. \tag{17}$$

Other components of the tensor $\delta\gamma(np\rightarrow p)$ can be obtained by cyclic permutations of x, y, and z indices. I_{np} is defined by Eq. (A9) in the Appendix, but note that the relative correction $\delta\gamma/\gamma^0$ involves only the occupation numbers $n_{np\kappa}$, while I_{np} cancels out. In the next section we turn to a more detailed discussion of various aspects of the EFG's measured in HTSC's. The scalar part of γ will be left as the free parameter, the same for all materials, to be determined from experimental data. Therefore, I_{np} and the solutions of Eq. (A6) are not relevant to this discussion.

The potential importance of the tensorial nature of γ can be appreciated through Eq. (17), i.e., for p orbitals. Assuming, e.g., that the occupied orbital is p_x, namely, $V_{yy}^{\rm local}=V_{zz}^{\rm local}$, but that $V_{\alpha\alpha}^{\rm lattice}$ is symmetric with respect to the y axis, $V_{xx}^{\rm lattice}=V_{zz}^{\rm lattice}$, it turns out in the calculation of Appendix A that $(\gamma V^{\rm lattice})_{yy}\approx-(\gamma V^{\rm lattice})_{zz}$. As argued below, such a strong tensorial character of γ is not found at the oxygen sites in high-T_c superconductors. Actually, at those sites the tensorial corrections of Eq. (17) will turn out to be negligible. The large tensorial corrections to the scalar value

TABLE II. The experimental EFG's (Refs. 4 and 8), the total lattice contributions to EFG and the estimated EFG's according to Eq. (18) (all in units of 10^{21} V/m^2), with the respective asymmetry parameters, for $La_{1.85}Sr_{0.15}CuO_4$. The effective charge of ions q_i and the number of holes in corresponding σ orbitals n_i are also done.

atom	V_{aa}	V_{bb} exp.	V_{cc}	η	η'	V_{aa}	V_{bb} lattice	V_{cc}	V_{aa}	V_{bb} Eq. (18)	V_{cc}	η	η'	q_i	n_i
O(1)	−1.0	−1.0	2.0	0		−0.52	−0.52	1.04	−1.04	−1.04	2.08	0		−1.96	0.04
O(2)	7.3	−5.0	−2.3	0.37	0.37	2.71	−2.0	−0.71	7.43	−4.36	−3.07	0.17	0.17	−1.82	0.18
Cu	7.0	7.0	−14.0	0		−2.47	−2.47	4.94	7.00	7.00	−14.00	0		1.71	0.71
La[a]						8.38	8.38	−16.76	8.38	8.38	−16.76	0		2.925	0

[a]In the calculation of the $V_{\alpha\alpha}^{\text{lattice}}$ contributions, the spatially averaged charge on La sites is used to insure the charge neutrality of the system. In Ref. 25 $V_{cc}=\pm 16.7\times 10^{21}$ V/m^2 at the La site in $La_{2-x}Sr_xCuO_4$, $x<0.08$, is reported.

of γ do occur, however, at the in-chain copper site of $YBa_2Cu_3O_7$, where they presumably involve the d states. The corresponding generalization of Eq. (17) is straightforward and will not be discussed here.

III. COMPARISON WITH EXPERIMENTS

First we consider the tensorial corrections $\delta\gamma(np\rightarrow p)$ at the oxygen sites, for the situation relevant here, when the occupation numbers per spin are approximately $n_{npy}=n_{npz}=0$ and $n_{npx}=0.1$. The following results are obtained: $\delta\gamma_{xx}=4\delta\gamma_{yy}=4\delta\gamma_{zz}=-0.066\gamma^0$, $\delta\gamma_{xy}=\delta\gamma_{xz}=0$, and $\delta\gamma_{zx}=-\delta\gamma_{zy}=\delta\gamma_{yx}=-\delta\gamma_{yz}=0.017\gamma^0$. Therefore, allowing for uncertainties in the calculation of the indirect lattice contribution of the order of a few percents, we may continue the EFG analysis by omitting the tensorial corrections at the oxygen sites. At the copper sites, the closed $3p$ subshell gives a dominant contribution to γ^0. The $\delta\gamma(3p\rightarrow p)$ correction disappears according to Eq. (A11). Moreover, in the tetragonal lattice of La_2CuO_4 compounds, where the hole distribution at the in-plane copper and respective $V_{\alpha\alpha}^{\text{lattice}}$ have fourfold symmetry, the total γ is strictly a scalar.

In what follows, the scalar values of γ will be labeled by γ(Cu), γ(O), γ(Ba), and γ(La), and the simplified version of Eq. (1) (γ scalar) to be used is

$$V_{\alpha\alpha}=(1-R)V_{\alpha\alpha}^{\text{local}}+(1-\gamma)V_{\alpha\alpha}^{\text{lattice}}. \tag{18}$$

The factor γ(Cu) is usually estimated by fitting the EFG measured at the in-chain Cu nuclei in insulating $YBa_2Cu_3O_6$. Since at this copper ion there are no holes, γ(Cu) is the only free parameter in Eq. (18). Assuming the stoichiometric valences of all ions except for the in-plane ones, $\gamma(\text{Cu})=-5.24$ is obtained. Further, when γ(Cu) and the in-plane doping level δ in $La_{2-x}Sr_xCuO_4$ are known, two remaining unknown quantities, γ(O) and the number of holes on the in-plane copper (or the in-plane oxygen) ion, can be easily estimated from EFG data. The value $\gamma(\text{O})=-6$ is obtained in this way. The values $\gamma(\text{Ba})=-62$ and $\gamma(\text{La})=-83$ also result directly from the experimental EFG.

Our next task is to test the possibility that some other orbitals except for σ ones are involved in bands near the Fermi energy. We focus our attention on the three materials for which the NMR/NQR measurements are available both at all oxygen and at all copper sites, namely, $La_{2-x}Sr_xCuO_4$, $YBa_2Cu_3O_7$, and $Tl_2Ba_2CuO_6$.[1–4,11,12] The assumption that only the σ orbitals are partially occupied corresponds to a particular form of the local charge distribution (LCD). Through Eq. (18), this LCD can be checked against experimental EFG's. For the parameters γ, R, and $\langle 1/r^3\rangle$, we use the values discussed previously. The only free parameter per site, the population of the respective σ orbital n_i, is estimated from the largest EFG component measured at the particular site. The validity of initial assumption is then tested on comparing the experimentally measured asymmetry parameter η to the one which corresponds to the assumed LCD. The results obtained by this procedure are shown in Tables II and III, and discussed below. In those tables the effective charge of an ion is equal:

$$q_i=q_i^0+2n_{nl\kappa}=q_i^0+n_i. \tag{19}$$

TABLE III. $YBa_2Cu_3O_7$: The experimental EFG's are from Refs. 1 and 2.

atom	V_{aa}	V_{bb} exp.	V_{cc}	η	η'	V_{aa}	V_{bb} lattice	V_{cc}	V_{aa}	V_{bb} Eq. (18)	V_{cc}	η	η'	q_i	n_i
Cu(2)	6.2	6.2	−12.4	0		−2.70	−2.00	4.70	5.83	6.54	−12.37	0.06		1.64	0.64
O(2)	10.5	−6.3	−4.1	0.20	0.20	2.97	−0.97	− 2.00	10.30	−4.64	−5.66	0.10	−0.10	−1.72	0.28
O(3)	−6.3	10.2	−3.9	0.23		−0.55	2.25	−1.70	−4.22	9.60	−5.38	0.12		−1.72	0.28
Ba[a]						−8.86	0.53	8.33	−8.86	0.53	8.33	0.88		2	0
O(1)	−4.0	−7.6	11.6	0.31		−0.51	−2.19	2.70	−4.31	−6.00	10.31	0.16		−1.71	0.29
Cu(1)	−7.4	7.5	0.0	0.99		7.77	−2.48	−5.29	−6.62	4.72	1.90	0.43		1.54	0.54
O(4)	−5.1	17.3	−12.1	0.4		−0.58	3.78	−3.20	−6.87	16.37	−9.50	0.16		−1.52	0.48
Y[b]						0.065	0.11	−0.175	0.065	0.11	−0.175	0.26		3	0

[a]We take that the experimental values from Ref. 26 correspond approximately to the antisymmetric EFG tensor with values (−8.7, 0, 8.7).
[b]We give here only the bare lattice contribution, because there are no $I>1/2$ Y nuclei.

Here q_i^0 is the charge of the ion in the vacuum state. In particular, for the in-plane copper and oxygen ions $q_{cu(2)} = 1 + n_d$, $q_{o(2)} = -2 + n_p$. A widely accepted notation is used here, n_d and n_p being the number of holes in the $3d_{x^2-y^2}$-Cu(2) and the $2p_\sigma$-O(2,3) orbitals, respectively.

A. Apex oxygen atom O(1)

The apex oxygen NMR presents a sensitive probe of the hybridization between O(1)-$2p_z$ and the in-plane copper orbitals.

Due to the small value of the O(1) EFG in $La_{2-x}Sr_xCuO_4$, our analysis gives a population of the O(1)-$2p_z$ orbital by holes less than 1/5 of the respective n_p. On the other hand, the crucial experimental observation is that, within the experimental resolution, the O(1) EFG is not changed by strontium dopings 0.075, 0.15, and 0.24.[4,13] This rules out a sizable participation of the O(1)-$2p_z$ orbital at the Fermi level in $La_{2-x}Sr_xCuO_4$, at least in the range of dopings mentioned above.

In contrast to that, in two other materials the estimated number of holes at the apex oxygen is comparable to the n_p, pointing to the strong hybridization of the O(1)-$2p_z$ orbital with the suitably oriented orbitals from the surrounding ions. Unfortunately, at present there are no measurements of the doping dependence of O(1) NMR spectra in these two families. It should be noted, however, that in $YBa_2Cu_3O_7$ the spacing between O(1) and Cu(1) sites is somewhat shorter than the distance between O(1) and Cu(2) (1.85 vs 2.29 Å). This supports the idea that the charge distribution responsible for EFG at O(1) is preferably related to the O(1)-$2p_z$ - Cu(1)-$3d_{y^2-z^2}$ hybridization rather than to the O(1)-$2p_z$ - Cu(2)-$3d_{3z^2-r^2}$ hybridization. This also agrees with the band structure results reported by Massidda *et al.*[27] It is even more likely that such a situation occurs in $Tl_2Ba_2CuO_6$. The Cu-O(1) distance is significantly increased there, d [Cu-O(1)] ≈ 2.7 Å, while d [Tl-O(1)] ≈ 1.98 Å is much smaller. Finally, it is interesting to note that the nonzero value of the asymmetry parameter η observed at O(1) in $YBa_2Cu_3O_7$ arises mostly from the presence of the in-chain oxygen ions. The orthorhombic distortion of the tetragonal lattice has only a small influence on η. Indeed, on assuming that the local contribution is unchanged by the orthorhombic distorsion, we obtain $\eta_O \approx 0.16$ and $\eta_T \approx 0.18$ for the orthorhombic and tetragonal lattice, respectively. More generally, experimentally measured small displacements of ions from their positions in the idealized lattices cause relatively small changes in $V_{\alpha\alpha}^{\text{lattice}}$ for nearby nuclei. This contrasts with much stronger effects of interstitial impurities [for example, the effect of the in-chain O(4) ion in $YBa_2Cu_3O_{6+x}$] on EFG.

B. In-plane oxygen atoms O(2,3)

In the conventional description of the symmetry of EFG through η one item of information, important to our discussion of O(2) EFG, remains hidden. This is best seen through the parameter $\eta' = (V_{cc} - V_{bb})/V_{aa}$. Clearly, $|\eta'|$ is equal to the asymmetry parameter η, but the sign of η' will turn out to distinguish between the asymmetries originating from the lattice and from the local EFG term.

At first sight the measured asymmetry parameters at O(2) ions are confusing. In spite of the fact that the neighborhood of the O(2) ion has a higher symmetry for the $La_{2-x}Sr_xCuO_4$ lattice than for $YBa_2Cu_3O_7$, the asymmetry parameter η is found to be larger in the former case. This issue has been previously discussed by Hanzawa *et al.*[16] However, as their model neglects the lattice contributions to EFG, it turns out to be inappropriate for the discussion of the EFG's for most of the out-of-plane ions. It is also too crude to satisfactorily explain η' at the O(2,3) positions. The experimental values of η' in $La_{2-x}Sr_xCuO_4$ and $YBa_2Cu_3O_7$ are $\eta' \approx 0.4$ and $\eta' \approx 0.2$, while the p_σ model predictions are $\eta' \approx 0.2$ and $\eta' \approx -0.1$ (see Tables II and III). In order to understand this discrepancy, it should be noted that, due to the a-axis uniaxial symmetry of the $2p_\sigma$ orbital at the O(2) site, the corresponding local contribution cancels out in the numerator of η'. The sign of η' is thus entirely determined by the lattice contribution in the assumed p_σ model. Therefore, we recalculated the lattice contribution in $YBa_2Cu_3O_7$ beyond the point charge approximation. The charge distribution on the neighboring ions was modeled by the Slater-type wave functions with parameters ζ_{2p} and ζ_{3d} given after Eq. (15). However, the correction to η' introduced in this way was not qualitatively significant, since η' remained negative. The solution of the problem comes on noting that the crystal field in the z direction admixes the $2p_z$ orbital to the wave function at the O(2) site of $YBa_2Cu_3O_7$. This admixture breaks the a-axis uniaxial symmetry of the contribution $V_{\alpha\alpha}^{\text{local}}$ in Eq. (18) and contributes a positive term to η'. It should be emphasized that the effect occurs through $V_{\alpha\alpha}^{\text{local}}$, rather than through the tensorial corrections to $\gamma V_{\alpha\alpha}^{\text{lattice}}$, which are neglected according to the discussion at the beginning of this section. The estimated occupation of the $2p_z$ orbital by holes required to give the experimental η' is somewhat less than 0.1 (while $n_{2p\sigma} \approx 0.3$). This agrees qualitatively with the result of the band calculation for EFG, reported by Schwarz *et al.*[14]

In contrast to $YBa_2Cu_3O_7$, the CuO_2 plane in the HTT phase of $La_{1.85}Sr_{0.15}CuO_4$ is a mirror symmetry plane. The crystal field in the z direction is absent, and therefore, at room temperature, there is no $2p_z$ admixture at the O(2) site. Only the lattice contributes a term to η', which is positive.

The structural phase transition between the high-temperature tetragonal (HTT) phase and a low-temperature orthorhombic (LTO) phase occurs at about 200 K in $La_{1.85}Sr_{0.15}CuO_4$. In the LTO phase (where the data given in Table II are taken), a tilting of the CuO_6 octahedra breaks (weakly) the mirror symmetry at the O(2) site. The resulting expectedly small $2p_z$ contribution is positive. It combines with the already positive value associated with the lattice. Hence, in contrast to $YBa_2Cu_3O_7$, the $2p_z$ contribution in $La_{2-x}Sr_xCuO_4$ is not of qualitative importance in explaining the sign of η'. On the other hand, the absence of EFG data through the HTT/LTO transition makes a quantitative comparison between experiment and theory premature. However, it can be safely concluded that the opposite signs of local and lattice contributions to η' in $YBa_2Cu_3O_7$ are responsible for a somewhat smaller positive value of η', observed in this material, than that in $La_{1.85}Sr_{0.15}CuO_4$.

The transition of the LTO phase into a low-temperature tetragonal (LTT) phase in $La_{2-x}Ba_xCuO_4$ introduces the mirror symmetry at one of the two in-plane oxygen sites,

TABLE IV. Optimally doped orthorhombic $Tl_2Ba_2CuO_{6+x}$ with $T_c \approx 85$ K, Refs. 11 and 12.

Atom	V_{aa}	V_{bb} exp.	V_{cc}	η	η'	V_{aa}	V_{bb} lattice	V_{cc}	V_{aa}	V_{bb} Eq. (18)	V_{cc}	η	η'	q_i	n_i
Cu [a]						−3.18	−3.18	6.36	4.56	4.56	−9.12	0		1.58	0.58
O(2)	12.2	−8.3	−3.9	0.36	0.36	3.56	−3.46	−0.10	12.08	−7.72	−4.36	0.28	0.28	−1.675	0.325
O(3)	−8.3	12.2	−3.9	0.36		−3.46	3.56	−0.10	−7.72	12.08	−4.36	0.28		−1.675	0.325
Ba						2.29	2.29	−4.58	2.29	2.29	−4.58	0		2	0
O(1)	−7.7	−7.7	15.4	0		−1.71	−1.71	3.42	−7.50	−7.50	15.00	0		−1.56	0.44
Tl [b]						0.40	0.40	−0.80	0.40	0.40	−0.80	0		2.215	1.215
O(4)	−4.3	−3.7	8.1	0.07		−1.45	−1.45	2.90	−4.47	−4.47	8.94	0		−1.77	0.23

[a]The value of $^{63}\nu_{Q,m} \approx 23.3$ MHz is measured, which corresponds to $V_{cc} = -9.1 \times 10^{21}$ V/m^2 and $\eta = 0$.
[b]The bare lattice contribution only is given here.

which forbids the $2p_z$ admixture at this site. There is, however, a charge transfer between the two oxygen sites in question.[29] Unfortunately, there is also a lack of experimental data for this interesting situation.

All qualitative arguments, mentioned for the LCD at O(2) in the HTT phase of $La_{1.85}Sr_{0.15}CuO_4$, hold in $Tl_2Ba_2CuO_6$ as well, as easily seen in Table IV.

C. In-plane copper atom Cu/Cu(2)

First we consider the symmetry of the LCD on copper ions, by analyzing the doping dependence of the main ^{63}Cu-NQR signal in $La_{2-x}Sr_xCuO_4$ (Fig. 1). On assuming that the occupation of both relevant orbitals $3d_{x^2-y^2}$ and $3d_{3z^2-r^2}$ changes with doping, the change of V_{zz} must be proportional to the difference $n(3d_{x^2-y^2}) - n(3d_{3z^2-r^2})$. This is because the $C^{l\kappa}_{\alpha\alpha}$ factors (Table I) for the respective orbitals are equal in magnitude but opposite in sign. At the same time, the lattice contribution to η in Eq. (11) is not appreciably affected by doping. As easily seen from the observed increase of $^{63}\nu_{Q,m}$ (Fig. 1), the excess charge going to the $3d_{3z^2-r^2}$ state is, within the limits of accuracy of the present analysis, at most ten percent of the charge which goes to the $3d_{x^2-y^2}$ state, contrary to the proposal that the excess charge on Cu is small and that its change with doping is mostly associated with the change of the $3d_{3z^2-r^2}$ occupation.[30] If this latter assumption were true, $^{63}\nu_{Q,m}$ would *decrease* slowly upon doping, contrary to observation.

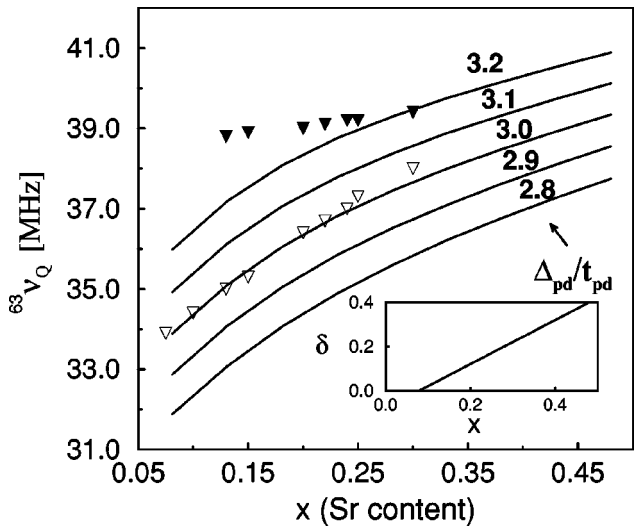

FIG. 1. The calculated dependence of the $^{63}\nu_Q$ frequency on x (full line), compared with the frequencies of the main and secondary ^{63}Cu-NQR signals ($^{63}\nu_{Q,m}$ and $^{63}\nu_{Q,s}$, labeled by open and filled triangles, respectively) measured in $La_{2-x}Sr_xCuO_4$, Ref. 8. (For $^{63}\nu_Q$ given in MHz units and V_{zz} in 10^{21} V/m^2 holds $^{63}\nu_Q = 2.55V_{zz}$.) Inset of figure shows relation δ to x.

In most compounds which belong to the three families under consideration, ^{63}Cu-NQR exhibits two signals attributed to the in-plane copper nuclei.[8,11,24] The origin of the splitting of these signals is not entirely clear and represents an interesting open question.

For example, the ^{63}Cu-NQR spectra in all La_2CuO_4-like compounds, $La_{2-x}Sr_xCuO_4$, $La_{2-x}Ba_xCuO_4$, and La_2CuO_{4+x}, are characterized by two signals.[7,8,28,31,32] Both signals are coming from the copper ions in the metallic regions of the sample. The frequencies measured in $La_{2-x}Sr_xCuO_4$ (Ref. 8) are shown in Fig. 1. In extended x-ray-absorption fine structure experiments[6] on $La_{1.85}Sr_{0.15}CuO_4$, two different copper sites are also found, one regular, and the other corresponding to the deformed CuO_6 octahedra. Taking into account the variation of $V^{\text{lattice}}_{\alpha\alpha}$ in this deformation, we find that the measured $^{63}\nu_Q$ frequences require the copper orbital occupancies $n_{d,m} \approx 0.71$ for the main and $n_{d,s} \approx 0.74$ for the secondary signal.

Next we turn to $YBa_2Cu_3O_{7-x}$ family where Cu-NQR spectra are the simplest and the best understood. Generally, two kinds of Cu(2) sites appear in the NQR spectra. The first site corresponds to the Cu(2) ion with neighboring in-chain O(4) oxygen positions empty, as in $YBa_2Cu_3O_6$, while for the second Cu(2) site these positions are occupied by oxygen ions.[33] In stoichiometric compounds only one Cu(2) site ap-

TABLE V. Distribution of the additional holes in $YBa_2Cu_3O_7$ ($\Delta_{pd} \approx 2t_{pd}$) and La_2CuO_4 ($\Delta_{pd} \approx 3t_{pd}$) based materials. δ is the doping of the plane obtained in the EFG analysis. In $YBa_2Cu_3O_6$ n_d is obtained using the experimental EFG, Ref. 24, while n_p follows after the assumption that $\delta = 0$.

	n_p	n_d	n_p^{add}	n_d^{add}	δ
$YBa_2Cu_3O_6$	0.225	0.55			0.0
$YBa_2Cu_3O_7$	0.28	0.64	27.5 %	45 %	0.2
$La_{1.85}Sr_{0.15}CuO_4$	0.18	0.71			0.07
$La_{1.76}Sr_{0.24}CuO_4$	0.215	0.73	39 %	22 %	0.16

pears: the first one in the insulating $YBa_2Cu_3O_6$ and the second one in metallic $YBa_2Cu_3O_7$. The Cu(2) EFG in $YBa_2Cu_3O_7$ is consistent with a local charge distribution where holes reside only in $3d_{x^2-y^2}$ orbital. There are some data related to the doping dependence of Cu-NQR spectra in the $YBa_2Cu_3O_7$ family, but they have been obtained by different authors on samples from different batches. Thus, we are unable to compare further the contributions of $3d_{x^2-y^2}$ and $3d_{3z^2-r^2}$ orbitals by repeating the argument used for the main ^{63}Cu-NQR signal in $La_{2-x}Sr_xCuO_4$. Neither Cu(2) EFG nor O(1) EFG give any clue about the degree of hybridization between O(1)-$2p_z$ and Cu(2)-$3d_{3z^2-r^2}$ orbitals in $YBa_2Cu_3O_{7-x}$. In $YBa_2Cu_3O_6$ the structure of EFG at the Cu(2) position is qualitatively similar to that in $YBa_2Cu_3O_7$. The quantitative doping dependence will be analyzed in next section (results are given in Table V).

In the orthorhombic phase of $Tl_2Ba_2CuO_{6+x}$ two $^{63}\nu_Q$ signals, split by 2–3 MHz, are found,[12] while in the tetragonal phase only one signal is observed. Shimakawa[34] did a chemical and structural study for various tetragonal and orthorhombic $Tl_2Ba_2CuO_{6+x}$ materials in order to find a possible relation between structural properties and the NQR observations. He suggests that the splitting of the $^{63}\nu_Q$ signals may be caused by the displacements of Tl ions from their ideal positions in the orthorhombic phase. We calculated corrections to $^{63}\nu_Q$ coming from these displacements as well as from displacements of oxygen ions from the TlO planes, present in both phases. The obtained differences in $^{63}\nu_Q$ for both kinds of lattice displacements are less than 1/10 of a percent. It seems that some kind of in-plane charge transfer, leading to two different n_d's, is needed in order to explain two ^{63}Cu-NQR signals in $Tl_2Ba_2CuO_{6+x}$.

D. In-chain copper atom Cu(1)

The most striking discrepancy between predictions with a scalar γ and experimental data is found at the in-chain copper site of $YBa_2Cu_3O_7$. The experimental EFG tensor is antisymmetric ($\eta \approx 1$), while the scalar Eq. (18) gives $\eta \approx 0.43$. The two terms which contribute to the expression (18) have significantly different symmetries: the local term, due to the corresponding σ orbital $3d_{y^2-z^2}$, and the bare lattice contribution have $(V_{bb}^{\rm local}-V_{cc}^{\rm local})/V_{aa}^{\rm local}=0$, and $(V_{bb}^{\rm lattice}-V_{cc}^{\rm lattice})/V_{aa}^{\rm lattice}\approx 0.36$, respectively. Thus, the precise calculation of the $(\gamma V^{\rm lattice})_{\alpha\alpha}$ at this crystal site must take into account the tensorial corrections to γ, presumably other $3d$ orbitals besides the $3d_{y^2-z^2}$ one, as already mentioned at the end of Sec. II.

To conclude, a variety of information related to EFG's measured in the HTSC materials was discussed. Only the symmetry-based conclusions can be accepted without reservation, while the others are more parameter dependent. Nevertheless, most of the parameter-dependent estimates, collected in Tables II–IV, may be submitted to further theoretical analysis. As a first step, and the simplest test of the EFG analysis, the charge neutrality of a unit cell can be checked for the materials where all ionic charges are estimated independently. At present this was done for $YBa_2Cu_3O_7$ and $Tl_2Ba_2CuO_{6+x}$, giving some additional, although rough support to our results of the EFG analysis.

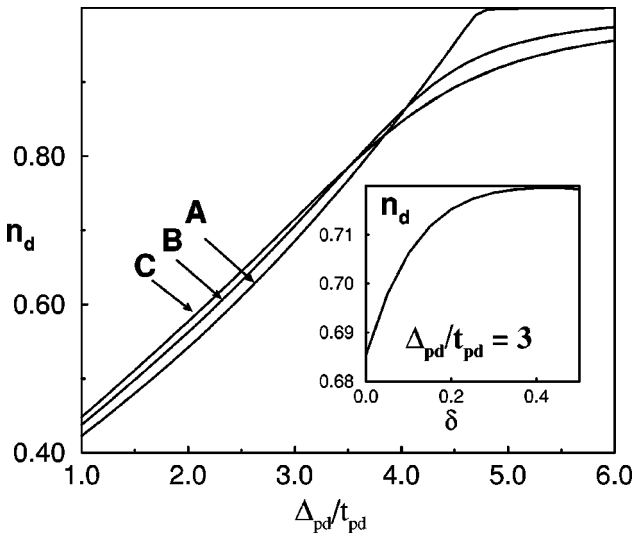

FIG. 2. The dependence of n_d on energy difference Δ_{pd} (main figure) for $\delta = 0.001$ (A), 0.1 (B), and 0.2 (C) and on doping δ (inset) in the regime of parameters which is appropriate to the La_2CuO_4 based materials.

IV. MANY-BODY MODEL

It is interesting to investigate finally how our results relate to models describing the correlated electrons in the cuprates.[29]

We start with Table V where the in-cell charge distributions for a pair of La_2CuO_4 and a pair of $YBa_2Cu_3O_7$ based materials is given. Note that in both families the holes doped into CuO_2 planes are shared in nearly equal proportions by copper and oxygen ions. At this point it should be recalled that there are numerous indications that the strong on-site repulsion U_d at the in-plane copper atom is important for the physics of cuprates. In particular, in the qualitative picture of the antiferromagnetic state the spin is entirely attributed to a singly occupied copper orbital. Therefore, it seems surprising that a large portion of the additional hole goes to the copper site. Moreover, our discussion of NQR data through Eq. (18) showed that, indeed, the pd model[35] takes into account all qualitatively important tight-binding states. The question which remains is whether the EFG results can be reconciled with the large U_d assumption in this model. We examine this question starting from the pd Hamiltonian

$$
\begin{aligned}
H=&\sum_{s\sigma}\left[E_d d_{s\sigma}^{\dagger}d_{s\sigma}+E_p(p_{xs\sigma}^{\dagger}p_{xs\sigma}+p_{ys\sigma}^{\dagger}p_{ys\sigma})\right]\\
&+\sum_{s\sigma}\left[t_{pd}(p_{xs\sigma}^{\dagger}+p_{ys\sigma}^{\dagger})d_{s\sigma}\right.\\
&\left.-t_{pd}(p_{xs-a\sigma}^{\dagger}+p_{ys-b\sigma}^{\dagger})d_{s\sigma}+\text{H.c.}\right]\\
&+\sum_{s}U_d d_{s\uparrow}^{\dagger}d_{s\uparrow}d_{s\downarrow}^{\dagger}d_{s\downarrow}\,. \qquad (20)
\end{aligned}
$$

Here $p_{xs\sigma}^{\dagger}$, $p_{ys\sigma}^{\dagger}$, and $d_{s\sigma}^{\dagger}$ are creation operators for holes in $2p_\sigma$-O(2), $2p_\sigma$-O(3), and $3d_{x^2-y^2}$-Cu(2) orbitals at the site s, respectively, while E_p and E_d are the corresponding on-site energies. The overlap energy between the first $2p_\sigma$ and $3d_{x^2-y^2}$ neighbors ($\pm t_{pd}$) is the only one taken into account.

As it is widely accepted that the on-site Coulomb repulsion U_p on the oxygen site is not a relevant parameter of the model, we use $U_p=0$. Furthermore, in order to simplify calculations, it is also usual to consider the model with the nearest and next nearest Coulomb interactions V_{pd} and V_{pp} equal to zero (some average shifts produced by these Coulomb terms are implicitly included in E_p and E_d).

For $U_d\to\infty$ the Hamiltonian (20) can be treated in the slave-boson approach,[36,37] using two auxiliary operators, fermionic $f^\dagger_{s\sigma}$ and bosonic $b^\dagger_s$. The first one represents a singly occupied $3d_{x^2-y^2}$ orbital at a site s while the other one represents the empty state—the electronic operator $d^\dagger_{s\sigma}$ becomes the composite object, $d^\dagger_{s\sigma}\equiv f^\dagger_{s\sigma}b_s$. The constraint $n_d\leqslant 1$ turns into equality $\Sigma_\sigma f^\dagger_{s\sigma}f_{s\sigma}+b^\dagger_s b_s=1$, when expressed in terms of the auxiliary operators. The constraint is then introduced into the Hamiltonian (20) through the respective Lagrange multipliers λ_s. On applying the saddle point approximation, $b^\dagger_s$ and λ_s are replaced by numbers b and λ. The Hamiltonian for fermions acquires the following form:

$$\begin{aligned}H-\mu N(1+\delta)=&\sum_{s\sigma}\,[(E_d+\lambda-\mu)f^\dagger_{s\sigma}f_{s\sigma}+(E_p-\mu)\\&\times p^\dagger_{xs\sigma}p_{xs\sigma}+(E_p-\mu)p^\dagger_{ys\sigma}p_{ys\sigma}]\\&+\sum_{s\sigma}\,b[t_{pd}(p^\dagger_{xs\sigma}+p^\dagger_{ys\sigma})f_{s\sigma}-t_{pd}\\&\times(p^\dagger_{xs-a\sigma}+p^\dagger_{ys-b\sigma})f_{s\sigma}+\text{H.c.}]\\&+\sum_s\,\lambda(b^2-1).\end{aligned}\tag{21}$$

λ and b have to be optimized by minimization of the thermodynamic potential Ω. After all the simplifications, the average charges in the copper and the oxygen orbitals depend only on two dimensionless parameters: doping of the conducting planes δ and Δ_{pd}/t_{pd}, the energy difference between $2p_\sigma$ and $3d_{x^2-y^2}$ levels ($\Delta_{pd}=E_p-E_d$) measured in terms of the pd overlap integral t_{pd}.

Since the EFG's are nearly independent of temperature, we solve the saddle point equations

$$\begin{aligned}\partial\Omega/\partial b&=0,\\ \partial\Omega/\partial\lambda&=0,\\ -\partial\Omega/\partial\mu&=N(1+\delta)\end{aligned}\tag{22}$$

at $T=0$ K. In Fig. 2 we show how the charge distribution, described in terms of the number of holes on the $3d_{x^2-y^2}$-Cu orbital, depends on two relevant parameters of the model, for δ = 0.001, 0.1, and 0.2 (main figure) and Δ_{pd} = 3.0 t_{pd} (inset).

Three qualitatively different regimes are found, $\partial n_d/\partial\delta>0$, $\partial n_d/\partial\delta\approx 0$, $\partial n_d/\partial\delta<0$, corresponding to $\Delta_{pd}/t_{pd}<4$, $\Delta_{pd}/t_{pd}\approx 4$, and $\Delta_{pd}/t_{pd}>4$, respectively. Although the estimated small values of additional n_d may be somewhat uncertain, on the qualitative side the results given in Table V ($\partial n_d/\partial\delta>0$) clearly show that the effective value of Δ_{pd} is comparable to the overlap integral t_{pd}. Besides, the other important qualitative result is the saturation of n_d with respect to the changes of δ or Δ_{pd}, already for not too large δ and Δ_{pd}. Such a saturation is the direct consequence of a large U_d.

In Fig. 1 we directly compare the results of the slave-boson calculation with the measured NQR spectra in $La_{2-x}Sr_xCuO_4$ materials. The dependence of resonant frequencies $^{63}\nu_Q$ on x confirms qualitatively the picture of a hole-doped pd model with large U_d and $\Delta_{pd}\sim t_{pd}$. Indeed, for chosen model parameters the holes doped into the conducting planes go to copper and oxygen sites in nearly equal proportions.

APPENDIX: CALCULATION OF $\gamma(np\to p)$

The quadrupolar part of the crystal potential acts as a perturbation on the unperturbed orbitals $\Psi^0_{np\kappa}(\mathbf{r})=(1/r)u^0_{np}(r)f_{p\kappa}(\Omega)$, with the respective orbital energy E_0. Here $u^0_{np}(r)=rR_{np}(r)$. In general, the quadrupolar potential is of the form

$$V^{\text{lattice}}=\frac{1}{4}[(3z^2-r^2)+\eta(x^2-y^2)]V^{\text{lattice}}_{zz},\tag{A1}$$

where η and the local axes are defined by Eq. (11). Considering only the radial polarizability of the p orbitals, the perturbed wave function can be written as

$$\begin{aligned}\Psi_{np\kappa}(\mathbf{r})&=\Psi^0_{np\kappa}(\mathbf{r})+\Psi^{(1)}_{np\kappa}(\mathbf{r})\\&=\frac{1}{r}[u^0_{np}(r)+B_{p\kappa}u^{(1)}_{np}(r)]f_{p\kappa}(\Omega).\end{aligned}\tag{A2}$$

In the first order of perturbation theory, the equation for $\Psi^{(1)}_{np\kappa}(\mathbf{r})$ takes the form

$$(H_0-E_0)|\Psi^{(1)}_{np\kappa}\rangle=[E^{(1)}_{np\kappa}-(-e)V^{\text{lattice}}]|\Psi^0_{np\kappa}\rangle.\tag{A3}$$

The energy corrections $E^{(1)}_{np\kappa}$ are

$$\begin{aligned}E^{(1)}_{npx}&=\frac{1}{5}\langle r^2\rangle_{np}(1-\eta)V^{\text{lattice}}_{zz},\\ E^{(1)}_{npy}&=\frac{1}{5}\langle r^2\rangle_{np}(1+\eta)V^{\text{lattice}}_{zz},\\ E^{(1)}_{npz}&=-\frac{2}{5}\langle r^2\rangle_{np}V^{\text{lattice}}_{zz}.\end{aligned}\tag{A4}$$

(Following Ref. 19 we use Rydberg atomic units.) The coefficients $B_{p\kappa}$ are obtained on writing the expression (A3) in the $\mathbf{r}$ representation, and integrating over angular variables:

$$\begin{aligned}B_{px}&=-\frac{1}{5}(1-\eta)V^{\text{lattice}}_{zz},\\ B_{py}&=-\frac{1}{5}(1+\eta)V^{\text{lattice}}_{zz},\\ B_{pz}&=\frac{2}{5}V^{\text{lattice}}_{zz}.\end{aligned}\tag{A5}$$

The function $u^{(1)}_{np}(r)$ thus satisfies the equation

$$\left(-\frac{d^2}{dr^2}+\frac{2}{r^2}+V_0-E_0 \right) u_{np}^{(1)}=(r^2-\langle r^2\rangle_{np})u_{np}^0, \quad \text{(A6)}$$

which, in general, has to be solved numerically. Here V_0 is an effective on-site potential.

The corresponding indirect lattice contribution to EFG can be written in terms of tensor $\gamma(np\rightarrow p)$

$$V_{\alpha\alpha}^{\text{ind}}=-\sum_{\beta}\ \gamma_{\alpha\beta}(np\rightarrow p)V_{\beta\beta}^{\text{lattice}}, \quad \text{(A7)}$$

and, at the same time, using Eqs. (8), (14), and (A2) as

$$V_{\alpha\alpha}^{\text{ind}}=-I_{np}\sum_{\kappa}\ (1-n_{np\kappa})4B_{p\kappa}C_{\alpha\alpha}^{p\kappa}. \quad \text{(A8)}$$

In the last expression, we introduce

$$I_{np}=\int u_{np}^0(r)\overline{u_{np}^{(1)}}(r)r^{-3}dr, \quad \text{(A9)}$$

where $\overline{u_{np}^{(1)}}(r)$ is obtained from $u_{np}^{(1)}(r)$ by the orthogonalization over all occupied p states:[38]

$$\overline{u_{np}^{(1)}}(r)=u_{np}^{(1)}(r)-\sum_{n'}\ u_{n'p}^0(r)\int u_{np}^{(1)}(r')u_{n'p}^0(r')dr'. \quad \text{(A10)}$$

This allows us to express $\gamma(np\rightarrow p)$ in terms of the integral I_{np}. As the transformation between expressions (A7) and (A8) is not unique, because $V_{\alpha\alpha}^{\text{lattice}}$ must satisfy the Laplace equation, any term proportional to $\Sigma_\alpha V_{\alpha\alpha}^{\text{lattice}}$ can be added to the right-hand side of Eqs. (A7) or (A8). We use this freedom to minimize the off-diagonal components of the tensor $\gamma(np\rightarrow p)$.

In this way one obtains that $\gamma(np\rightarrow p)$ is a scalar for a closed-shell configuration, and equal to

$$\gamma^0(np\rightarrow p)=\frac{48}{25}I_{np}. \quad \text{(A11)}$$

The number 48/25 is the well-known Sternheimer's factor related to the closed p subshells.

For the partially filled shells, the result is

$$\gamma(np\rightarrow p)=\gamma^0(np\rightarrow p)+\delta\gamma(np\rightarrow p),$$

with $\delta\gamma$ given by Eq. (17) in the main text.

[1] M. Takigawa, P. C. Hammel, R. H. Heffner, Z. Fisk, K. C. Ott, and J. D. Thompson, Phys. Rev. Lett. **63**, 1865 (1989).

[2] C. H. Pennington, D. J. Durand, C. P. Slichter, J. P. Rice, E. D. Bukowski, and D. M. Ginsberg, Phys. Rev. B **39**, 2902 (1989).

[3] M. Horvatić, Y. Berthier, P. Butaud, Y. Kitaoka, P. Ségransan, C. Berthier, H. Katayama-Yoshida, Y. Okabe, and T. Takahashi, Physica C **159**, 68 (1989).

[4] K. Ishida, Y. Kitaoka, G.-Q. Zheng, and K. Asayama, J. Phys. Soc. Jpn. **60**, 3516 (1991).

[5] E. D. Isaacs, G. Aeppli, P. Zschack, S-W. Cheong, H. Williams, and D. J. Buttrey, Phys. Rev. Lett. **72**, 3421 (1994).

[6] A. Bianconi, N. L. Saini, A. Lanzara, M. Missori, T. Rossetti, H. Oyanaga, H. Yamaguchi, K. Oka, and T. Ito, Phys. Rev. Lett. **76**, 3412 (1996).

[7] H. Tou, M. Matsumura, and H. Yamagata, J. Phys. Soc. Jpn. **61**, 1477 (1992).

[8] S. Ohsugi, Y. Kitaoka, K. Ishida, G.-Q. Zheng, and K. Asayama, J. Phys. Soc. Jpn. **63**, 700 (1994).

[9] S. Shamoto, M. Sato, J. M. Tranquada, B. J. Sternlieb, and G. Shirane, Phys. Rev. B **48**, 13 817 (1993).

[10] J. M. Tranquada, B. J. Sternlieb, J. D. Axe, Y. Nakamura, and S. Ushida, Nature (London) **375**, 561 (1995).

[11] S. Kambe, H. Yasuoka, A. Hayashi, and Y. Ueda, Phys. Rev. B **47**, 2825 (1993).

[12] S. Kambe, H. Yasuoka, A. Hayashi, and Y. Ueda, in *Proceedings of the 2nd ISSP International Symposium*, Tokyo, Japan, 1991, *The Physics and Chemistry of Oxide Superconductors*, edited by Y. Iye and H. Yasuoka (Springer, Berlin, 1991), p. 361.

[13] G.-Q. Zheng, T. Kuse, Y. Kitaoka, K. Ishida, S. Ohsugi, K. Asayama, and Y. Yamada, Physica C **208**, 339 (1993).

[14] K. Schwarz, C. Ambrosch-Draxl, and P. Blaha, Phys. Rev. B **42**, 2051 (1990).

[15] T. Shimizu, J. Phys. Soc. Jpn. **62**, 772 (1993).

[16] K. Hanzawa, F. Komatsu, and K. Yosida, J. Phys. Soc. Jpn. **59**, 3345 (1990).

[17] I. Kupčić, S. Barišić, and E. Tutiš, J. Phys. I **6**, 2291 (1996).

[18] E. N. Kaufmann and R. J. Vianden, Rev. Mod. Phys. **51**, 161 (1979).

[19] R. M. Sternheimer, Phys. Rev. A **6**, 1702 (1972), and references therein.

[20] J. D. Jorgensen, B. W. Veal, A. P. Paulikas, L. J. Nowicki, G. W. Crabtree, H. Claus, and W. K. Kwok, Phys. Rev. B **41**, 1863 (1990).

[21] M. François, K. Yvon, P. Fisher, and M. Decroux, Solid State Commun. **63**, 35 (1987).

[22] F. Izumi, J. D. Jorgensen, Y. Shimakawa, Y. Kubo, T. Manako, S. Pei, T. Matsumoto, R. L. Hitterman, and Y. Kanke, Physica C **193**, 426 (1992).

[23] E. Clementi and D. L. Raimondi, J. Chem. Phys. **38**, 2686 (1963).

[24] H. Yasuoka, T. Imai, and T. Shimizu, *Strong Correlation and Superconductivity*, Vol. 89 of Springer Series in Solid-State Sciences (Springer, Berlin, 1989), p. 254.

[25] I. Watanabe, J. Phys. Soc. Jpn. **63**, 1560 (1994).

[26] A. Yakubovskii, A. Egorov, and H. Lütgemeier, Appl. Magn. Reson. **3**, 665 (1992).

[27] S. Massidda, J. Yu, and A. J. Freeman, Phys. Lett. A **122**, 198 (1987).

[28] P. C. Hammel, A. R. Reyes, S.-W. Cheong, and Z. Fisk, Phys. Rev. Lett. **71**, 440 (1993).

[29] S. Barišić and J. Zelenko, Solid State Commun. **74**, 367 (1990); S. Barišić, Int. J. Mod. Phys. B **5**, 2439 (1991).

[30] C. Di Castro, L. F. Feiner, and M. Grilli, Phys. Rev. Lett. **66**, 3209 (1991); L. F. Feiner, M. Grilli, and C. Di Castro, Phys. Rev. B **45**, 10 647 (1992).

[31] K.-I. Ueda, T. Sugata, Y. Kohori, T. Kohara, Y. Oda, M. Yamada, S. Kashiwai, and M. Motoyama, Solid State Commun. **73**, 49 (1990).

[32] K. Yoshimura, T. Imai, T. Shimizu, Y. Ueda, K. Kosuge, and H. Yasuoka, J. Phys. Soc. Jpn. **58**, 3057 (1989).
[33] S. Barišić, I. Kupčić, and I. Batistić, Int. J. Mod. Phys. B **3**, 2051 (1989).
[34] Y. Shimakawa, Physica C **204**, 247 (1993).
[35] V. J. Emery, Phys. Rev. Lett. **58**, 2794 (1987).
[36] G. Kotliar, P. A. Lee, and N. Read, Physica C **153-155**, 538 (1988).
[37] S. Barišić and E. Tutiš, Solid State Commun. **87**, 557 (1993).
[38] P. C. Schmidt, K. D. Sen, T. P. Das, and A. Weiss, Phys. Rev. B **22**, 4167 (1980).